Support Information for: CO_2 Dissolution Efficiency during Geological Carbon Sequestration (GCS) in Perfectly Stratified Aquifers

Yufei Wang[1,2] **Daniel Fernàndez-Garcia**[1,2] **Maarten W. Saaltink**[1,2]

[1]Dept. of Civil and Environmental Engineering, Universitat Politècnica de Catalunya, Jordi Girona 1-3, 08034 Barcelona, Spain
[2]Associated Unit: Hydrogeology Group (UPC-CSIC)

Corresponding author: Yufei Wang, yufei.wang@upc.edu

Abstract
This support information offers the saturation and concentration distributions for different cases.

Figures

Figure 1 shows the distributions of $CO_2(g)$ plumes and $CO_2(aq)$ concentrations for the real heterogeneous field when normal injection rate is employed.

Figure 2 shows the distributions of $CO_2(g)$ plumes and $CO_2(aq)$ concentrations for the real heterogeneous field when slow injection rate is employed.

Figure 3 illustrates distributions of $CO_2(g)$ saturation and $CO_2(aq)$ concentration for the representative formations with upscaled permeability when normal injection rate is employed.

Figure 4 illustrates distributions of $CO_2(g)$ saturation and $CO_2(aq)$ concentration for the representative formations with upscaled permeability when slow injection rate is employed.

Figure 5 shows the distributions of ensemble average saturation and ensemble average concentration for heterogeneous cases when normal injection rate is employed.

Remark

The distribution of dissolved $CO_2(aq)$ concentration in brine is closely related to that of $CO_2(g)$ saturation. Therefore, in the paper we only show the distribution of $CO_2(g)$ saturation.

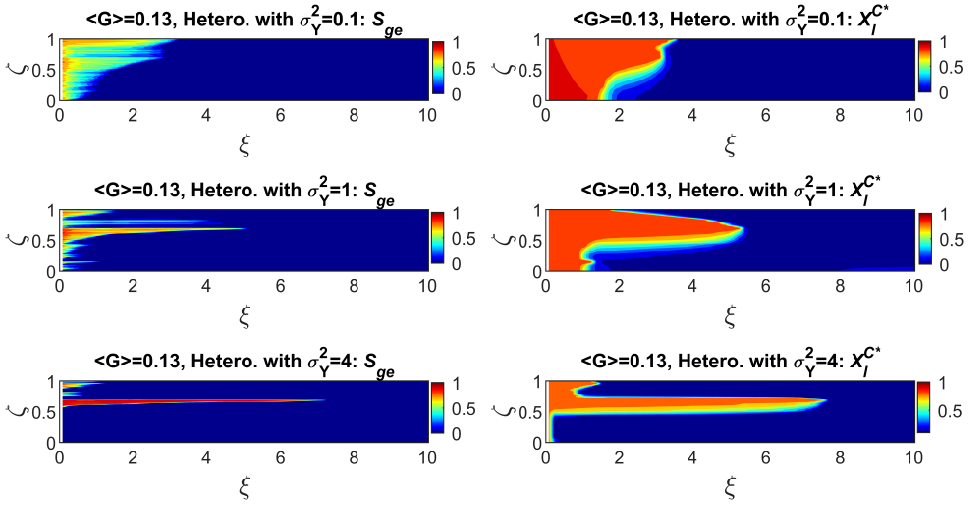

Figure 1: $CO_2(g)$ plumes (left column) and $CO_2(aq)$ concentrations in brine phase (right column) for the representative realization of the layered formations with σ_Y^2=0.1, 1, 4, respectively; normal injection rate Q_r=2.5 [Mt/year] is employed.

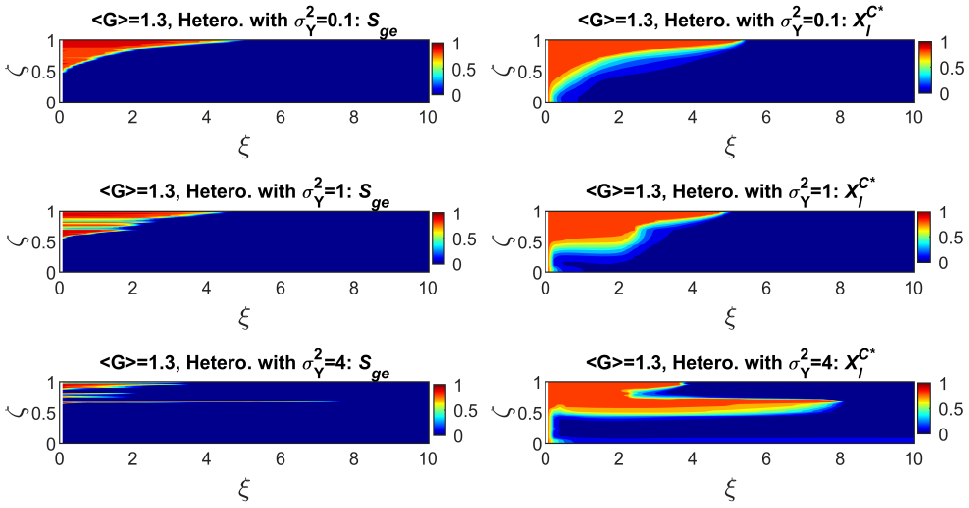

Figure 2: $CO_2(g)$ plumes (left column) and $CO_2(aq)$ concentrations in brine phase (right column) for the representative realization of the layered formations with σ_Y^2=0.1, 1, 4, respectively; slow injection rate Q_r=0.25 [Mt/year] is employed.

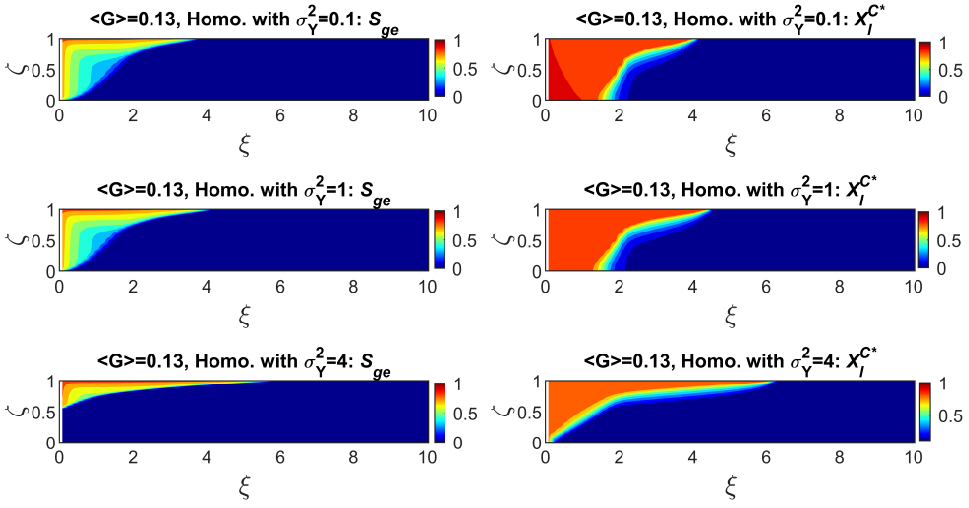

Figure 3: $CO_2(g)$ plumes (left column) and $CO_2(aq)$ concentrations in brine phase (right column) for representative formations with upscaled permeability corresponding to σ_Y^2=0.1, 1, 4, respectively; normal injection rate Q_r=2.5 [Mt/year] is employed.

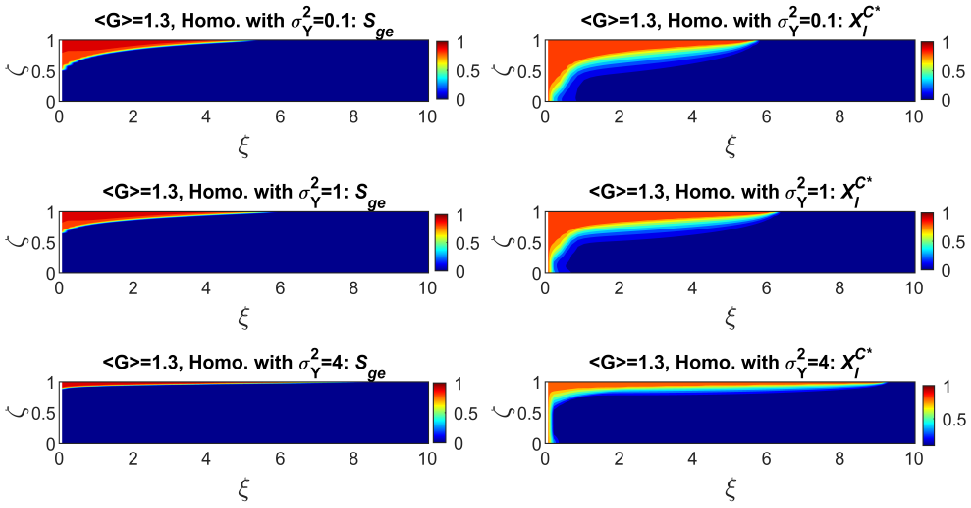

Figure 4: $CO_2(g)$ plumes (left column) and $CO_2(aq)$ concentrations in brine phase (right column) for representative formations with upscaled permeability corresponding σ_Y^2=0.1, 1, 4, respectively; slow injection rate Q_r=0.25 [Mt/year] is employed.

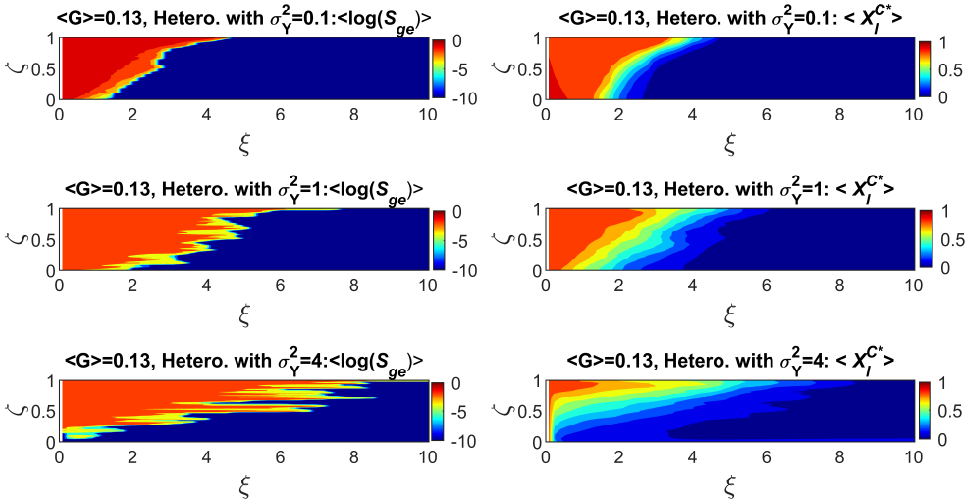

Figure 5: Ensemble averages of $CO_2(g)$ plumes (left column) and $CO_2(aq)$ concentrations in brine phase (right column) for the layered formations with σ_Y^2=0.1, 1, 4, respectively; normal injection rate Q_{well}=2.5 [Mt/year] is employed.